

OASIS: Harnessing Diffusion Adversarial Network for Ocean Salinity Imputation using Sparse Drifter Trajectories

Bo Li*

Griffith University
Gold Coast, Australia
bo.li6@griffithuni.edu.au

Yingqi Feng*

Florida Atlantic University
Boca Raton, USA
yfeng2016@fau.edu

Ming Jin

Xin Zheng
Griffith University
Gold Coast, Australia
{ming.jin,xin.zheng}@griffith.edu.au

Yufei Tang

Laurent Cherubin
Florida Atlantic University
Boca Raton, Fort Pierce, USA
{tangy,lcherubin}@fau.edu

Alan Wee-Chung Liew

Can Wang
Griffith University
Gold Coast, Australia
{a.liew,can.wang}@griffith.edu.au

Qinghua Lu

Data61, CSIRO
Alexandria, Australia
qinghua.lu@data61.csiro.au

Jingwei Yao

Griffith University
Gold Coast, Australia
jingwei.yao@griffithuni.edu.au

Shirui Pan

Hong Zhang
Griffith University
Gold Coast, Australia
{s.pan,hong.zhang}@griffith.edu.au

Xingquan Zhu

Florida Atlantic University
Boca Raton, USA
xzhu3@fau.edu

Abstract

Ocean salinity plays a vital role in circulation, climate, and marine ecosystems, yet its measurement is often sparse, irregular, and noisy, especially in drifter-based datasets. Traditional approaches, such as remote sensing and optimal interpolation, rely on linearity and stationarity, and are limited by cloud cover, sensor drift, and low satellite revisit rates. While machine learning models offer flexibility, they often fail under severe sparsity and lack principled ways to incorporate physical covariates without specialized sensors. In this paper, we introduce the **OceAn Salinity Imputation System (OASIS)**, a novel diffusion adversarial framework designed to address these challenges by: (1) employing a transformer-based global dependency capturing module to learn long-range spatiotemporal correlations from sparse trajectories; (2) constructing a generative imputation model that conditions on easily observed tidal covariates to progressively refine imputed salinity fields; and (3) using a scheduler diffusion method to enhance the model's robustness. This unified architecture exploits the periodic nature of tidal signals as a proxy for unmeasured physical drivers, without the need for additional equipment. We evaluate OASIS on four benchmark datasets, including one real-world measurement from Fort Pierce Inlet, Florida, USA and three simulated Gulf of Mexico trajectories.

*Both authors contributed equally to this work.

Results show consistent improvements over both traditional and neural baselines, achieving up to 52.5% reduction in MAE compared to Kriging. We also develop a lightweight, web-based deployment system that enables salinity imputation through interactive and batch interfaces, available at: <https://github.com/yfeng77/OASIS>.

CCS Concepts

• **Computing methodologies** → **Machine learning approaches**; **Modeling methodologies**; • **Information systems** → *Spatial-temporal systems*; • **Applied computing** → Earth and atmospheric sciences.

Keywords

Missing Data, Time Series, Imputation, Diffusion Adversarial Network, Salinity, Drifter

ACM Reference Format:

Bo Li, Yingqi Feng, Ming Jin, Xin Zheng, Yufei Tang, Laurent Cherubin, Alan Wee-Chung Liew, Can Wang, Qinghua Lu, Jingwei Yao, Shirui Pan, Hong Zhang, and Xingquan Zhu. 2025. OASIS: Harnessing Diffusion Adversarial Network for Ocean Salinity Imputation using Sparse Drifter Trajectories. In *Proceedings of the 34th ACM International Conference on Information and Knowledge Management (CIKM '25)*, November 10–14, 2025, Seoul, Republic of Korea. ACM, New York, NY, USA, 9 pages. <https://doi.org/10.1145/3746252.3761541>.

1 Introduction

Salinity, along with temperature and pressure, is a fundamental parameter for understanding the physical and chemical processes of the ocean [41]. It plays a key role in driving oceanic phenomena such as thermohaline circulation, water mass formation, and nutrient transport [4, 35, 44]. Therefore, understanding the spatial and temporal variability of salinity is essential for advancing marine science and managing marine resources.

Permission to make digital or hard copies of all or part of this work for personal or classroom use is granted without fee provided that copies are not made or distributed for profit or commercial advantage and that copies bear this notice and the full citation on the first page. Copyrights for components of this work owned by others than the author(s) must be honored. Abstracting with credit is permitted. To copy otherwise, or republish, to post on servers or to redistribute to lists, requires prior specific permission and/or a fee. Request permissions from permissions@acm.org.
CIKM '25, Seoul, Republic of Korea.

© 2025 Copyright held by the owner/author(s). Publication rights licensed to ACM.
ACM ISBN 979-8-4007-2040-6/2025/11
<https://doi.org/10.1145/3746252.3761541>.

Salinity in the open ocean is relatively conservative, primarily influenced by evaporation, precipitation, and currents [47, 51, 52]. In contrast, offshore and coastal waters exhibit significant salinity variability driven by freshwater inputs from river discharge, which dynamically interacts with tides, wind forcing, and human activities such as dam operations and land-use changes [34]. Due to their ecological sensitivity, economic importance, and high population density, these regions are particularly affected by salinity dynamics, which have direct implications for estuarine ecosystems, marine biodiversity, water quality, and the resilience of coastal infrastructure [37]. Therefore, this study focuses on the **salinity dynamics of nearshore waters** to improve our understanding of their controlling mechanisms and variability. It addresses the urgent need for robust and practical salinity estimation tools tailored to such complex nearshore environments.

Drifters equipped with hydrological sensors can be used to measure salinity along the drifter track. However, measurements obtained are often extremely sparse due to the separation between drifter trajectories. As a result, nearshore salinity modeling is naturally framed as an imputation task: estimating missing values at unobserved times and locations from limited, irregular drifter data. Previous studies have developed sea salinity imputation frameworks leveraging remote sensing and optimal interpolation techniques [9, 21, 32, 33]. However, these approaches assume spatial stationarity and linear dynamics, failing to capture fine-scale temporal variability due to cloud cover, sensor drift, and the limited revisit frequency of satellite instruments. Additionally, satellite-derived salinity is often noisy and depends heavily on in situ calibration and validation [6, 17]. Consequently, it is crucial to construct accurate imputation models capable of robust salinity interpolation. Recent data-driven approaches, from multilayer perceptrons (MLPs) [29] to deep neural models [19, 38], have been applied to salinity forecasting. Some incorporate covariates such as tides [13], yet most focus on forecasting rather than tackling sparse imputation or explicitly modeling spatiotemporal dependencies.

As promising generative models for imputation, Generative Adversarial Network (GAN) models have advanced substantially by learning to map random noise vectors to plausible data distributions. In the imputation context, GANs model the conditional distribution of missing values given observed data, allowing the generator to infer realistic and coherent imputations, while the discriminator distinguishes between observed and imputed entries. This architecture has inspired numerous imputation methods that leverage adversarial training to reconstruct missing values [2, 10, 14, 43, 46], making it an effective learning model for addressing the significant data sparsity challenge. Simultaneously, transformer architectures characterized by multi-head self-attention demonstrate exceptional capability in capturing global spatiotemporal dependencies, making them well suited for tasks requiring long-range interactions [42]. However, existing GAN-based imputation models often struggle with two key limitations in ocean applications: (1) insufficient capacity to capture long-range dependencies across sparse drifter tracks, and (2) instability or bias due to heterogeneous data distributions caused by drifting sensors and dynamic ocean conditions. These limitations motivate our design of a more robust, physically grounded imputation model tailored to coastal ocean salinity reconstruction.

In this work, we propose the **OceAn Salinity Imputation System (OASIS)**, a diffusion adversarial framework that integrates: **(1) Normalization Module** to remove distributional shifts across drifting sensors, ensuring stable training and reducing bias; **(2) Global Dependency Capturing (GDC)**: a transformer-based module that learns long-range spatial–temporal correlations from sparse drifter tracks; **(3) Scheduler Diffusion Adversarial Network (DAN)**: a generative adversarial network refined by a cosine-schedule noise diffuser and adversarial loss, conditioned on tidal height to progressively enhance imputation fidelity. Our key contributions are:

- (1) To the best of our knowledge, this work presents the first integration of generative sea salinity imputation into a fully automated framework tailored for sparse drifter trajectories.
- (2) Propose a unified architecture that addresses domain-specific challenges, such as sensor drift, data heterogeneity, and long-range dependencies, by integrating normalization, attention-based modeling, adversarial refinement, and a lightweight deployment component.
- (3) Compile four datasets spanning both simulated and real-world drifter trajectories with salinity data, covering diverse conditions and sparsity levels. These serve as benchmarks for ocean monitoring and data-driven environmental research.
- (4) Extensive experiments show that OASIS consistently outperforms existing baselines. On the real-world dataset, it reduces RMSE by 21.3% and MAPE by 18.5% over the best-performing baseline, demonstrating its robustness in realistic nearshore settings.
- (5) Develop a lightweight, extensible web-based system that enables real-time salinity imputation through interactive input and batch processing, enhancing accessibility for marine researchers and practitioners.

2 Related Work

2.1 Traditional Statistical Interpolation

Early ocean salinity imputation relied on Optimal Interpolation (OI) and Kriging methods, which effectively smoothed out the noise by maximizing the likelihood of fusing the observations with the background field. For OI, Fu et al. [11] describe the implementation of an Ensemble Optimal Interpolation (EnOI) in a two-way nested North/Baltic Sea model for assimilating temperature and salinity profiles. In terms of Kriging, Chen et al. [8] used a Kriging-based interpolation method to estimate the error of the Trophic State Index in Quanzhou Bay.

2.2 GAN-based Imputation

Missing data issues pervade a wide range of application domains, highlighting the extensive utility of data imputation models. Furthermore, several studies have leveraged industrial datasets to rigorously evaluate the performance of GAN-based imputation methods [2, 10, 18, 43, 46]. Traffic data imputation represents one of the most widely adopted applications of data imputation techniques. Guo et al. [14] evaluated several GAN-based models on spatiotemporal traffic datasets. Moreover, other studies have extended GAN-based imputation to domains such as finance [26], network measurement [39], cyber-attack analysis [7], and air quality monitoring [54].

2.3 Time Series Imputation

Time series imputation has long been a prominent research area, exploiting both temporal dependencies and inter-feature relationships to restore missing observations. Early approaches relied on statistical methods, such as last-observation carried forward and k -nearest neighbors imputation, to fill data gaps [3, 40]. Furthermore, a substantial body of work has leveraged Recurrent Neural Networks (RNNs) [22, 24, 30, 45] and Transformer-based architectures [49] to model temporal dependencies across diverse application domains [36, 50, 53], including healthcare [48], urban analytics [27], environmental monitoring [20], and indoor systems [28].

3 Methodology

The objective of sea salinity imputation is to reconstruct missing salinity values from sparse and irregularly sampled drifter trajectories. This task is crucial for supporting subsequent oceanographic analysis, particularly in coastal and offshore regions where data is limited and noisy. Traditional approaches, such as Kriging-based interpolation [8] and remote sensing retrievals, are constrained by strong stationary assumptions, low temporal resolution, and limited accuracy in coastal zones [25]. Statistical methods typically capture only spatial correlations and fail to model spatiotemporal interactions. Meanwhile, satellite-derived salinity products suffer from cloud occlusion, sensor drift, and infrequent revisits, and they are poorly suited to reconstructing fine-grained, transient ocean features. Moreover, drifter observations result in highly sparse and irregular data tensors, posing additional challenges to conventional interpolation schemes. Our OASIS overcomes these challenges in two ways. First, we integrate a transformer-based module into our architecture to capture global dependencies within the data (Section 3.3.1). Second, we employ a DAN model to enrich feature representations, reconstruct fine-grained local details, and perform the imputation task (Section 3.3.2).

3.1 Problem Statement

Drifter Data Representation. We represent our drifter data as a partially observed 4D tensor $\mathbf{X} \in \mathbb{R}^{T \times U \times V \times D}$, where T is the number of discrete time steps $\{t_1, t_2, \dots, t_T\}$, U, V are grid dimensions in latitude and longitude, and D is the number of sensor variables (e.g., salinity, temperature, pressure). The entry $\mathbf{X}(t, u, v, d)$ is the observed point of one drifter at time t and spatial cell (u, v) or NaN if missing. A corresponding mask $\mathbf{M} \in \{0, 1\}^{T \times V \times U \times D}$ indicates whether each entry is present (1) or missing (0) due to buoy sparsity. **Spatiotemporal Sea Salinity Imputation.** We consider K drifter trajectories that record D different sensor variables (e.g. tide height, salinity) over T discrete time-steps $\{t_1, \dots, t_T\}$. To enable joint spatiotemporal imputation, we overlay the study region with a regular grid of size $U \times V$ (latitude \times longitude) and aggregate all observations onto this grid. The result is a partially observed fourth-order tensor $\mathbf{X} \in \mathbb{R}^{T \times U \times V \times D}$. Our goal is to *impute salinity values at arbitrary times and locations* throughout the study area using a model trained on drifter-observed data, denoted as:

$$\hat{S} = f_{\theta}(t, u, v, d), \quad (1)$$

where $\hat{S} \in \mathbb{R}^{T \times U \times V}$ is the imputed salinity value at arbitrary times and locations in the study region.

3.2 Data Normalization

Although our study concentrates on a specific region, marine environmental conditions exhibit significant heterogeneity across different latitudes and longitudes. To mitigate this distribution shift, we employ the RevIN [23] to statistically influence in drifter data. For each drifter trajectory with M observations, we compute the mean μ and variance σ^2 as

$$\mu = \frac{1}{M} \sum_{i=1}^M \mathbf{X}_i, \quad \sigma^2 = \frac{1}{M} \sum_{i=1}^M (\mathbf{X}_i - \mu)^2. \quad (2)$$

We then normalize each observation \mathbf{X} and apply a learnable affine transformation:

$$\mathbf{X} = \gamma \left(\frac{\mathbf{X} - \mu}{\sqrt{\sigma^2 + \epsilon}} \right) + \beta, \quad (3)$$

where γ and β are initialized to 1 and 0, respectively, and are optimized during model training.

3.3 OASIS: Sea Salinity Imputation Under Sparse Drifter Data

3.3.1 Global Dependencies Capturing. For sea salinity imputation, the available inputs include temporal information, spatial locations (latitude \times longitude) and some observed covariate features we can get easily, like tide and depth. To cope with the first challenge which cannot be solved by general sea salinity imputation, we propose to utilize transformer-based module to capture the global temporal dependencies and in-channel interactions in the input feature sequences, which mainly consists of Positional Encoding (PE) and Multi-Head Self-Attention (MHA), and combines residual concatenation with layer normalization to stabilize the training. Since self-attention is inherently insensitive to sequence order [15], positional encoding needs to be injected for each time step. To incorporate positional information into each drifter embedding \mathbf{X} , we first augment it with a positional encoding $\mathbf{PE} \in \mathbb{R}^{N \times D}$, where $N = U \times V$:

$$\mathbf{X} = \mathbf{X} + \mathbf{PE}. \quad (4)$$

We then project \mathbf{X} into query, key, and value vectors using three learnable weight matrices W_Q, W_K , and W_V :

$$\mathbf{Q} = W_Q \mathbf{X}, \quad \mathbf{K} = W_K \mathbf{X}, \quad \mathbf{V} = W_V \mathbf{X}. \quad (5)$$

Finally, we compute scaled dot-product attention as

$$\text{Attention}(\mathbf{Q}, \mathbf{K}, \mathbf{V}) = \text{softmax} \left(\frac{\mathbf{Q}\mathbf{K}^T}{\sqrt{d_k}} \right) \mathbf{V}. \quad (6)$$

Hence, the attention score between position i and j is:

$$A_{i,j} = \frac{\exp(Q_i K_j / \sqrt{d_k})}{\sum_{j'=1}^N \exp(Q_i K_{j'} / \sqrt{d_k})}, \quad \mathbf{X}_i = \sum_{j=1}^N A_{i,j} \mathbf{V}_j, \quad (7)$$

which is a global dependency for position i to all position $j = \{1, 2, \dots, N\}$.

3.3.2 DAN-based Sea Salinity Imputation Model. Another challenge in sea salinity imputation based on drifter data is the inherent sparsity of observations. Because drifter trajectories do not provide dense coverage of the study area, we employ a DAN that refines GAN to mitigate this issue. On the one hand, GANs have demonstrated effectiveness in addressing data sparsity issues [1]. On the other hand, since the underlying distribution within a specific study

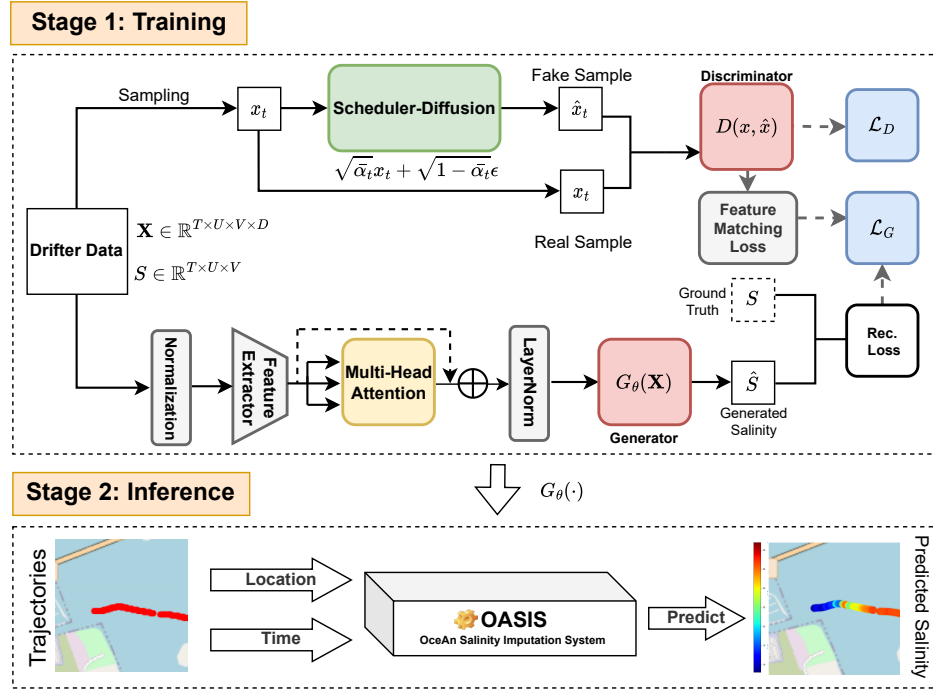


Figure 1: An overview of the two-stage pipeline for OASIS is detailed in Section 3: Stage 1 involves the model training process of OASIS. For the GENERATOR, it involves a normalization module described in Section 3.2, a Global Dependency Capturing module described in Section 3.3.1, and GENERATOR loss formulated by Eq. 11. In terms of DISCRIMINATOR, it involves SCHEDULER DIFFUSION module described in Section 3.3.2 and DISCRIMINATOR loss formulated by Eq. 9. Stage 2 is inference. For any time and location, OASIS can give an imputed sea salinity value.

region is expected to be relatively homogeneous, GANs can be trained to learn an ideal generative model capable of accurately imputing missing values [12].

In this section, the salinity imputation model based on the diffusion adversarial framework is proposed. The whole model consists of three core components: (1) a diffusion noise scheduler (SCHEDULER DIFFUSION), (2) a discriminator (DISCRIMINATOR), and (3) a generator (GENERATOR). During the training process, the DIFFUSION module is responsible for injecting multi-scale noise into real and fake samples, while the DISCRIMINATOR and GENERATOR are alternately optimized under the driving force of adversarial and feature matching, which ultimately enables the GENERATOR to accurately impute salinity values.

Scheduler Diffusion. We use a cosine scheduling strategy to design the forward diffusion process. Let T be the total diffusion steps, so at step t , the weight at this step would be $\beta_t = \beta_0 + \frac{1}{2}(\beta_T - \beta_0)(1 + \cos(\pi \frac{T-t}{T}))$, $\alpha_t = 1 - \beta_t$, $\bar{\alpha}_t = \prod_{i=1}^t \alpha_i$. Hence, for any input x_t , through noise $\epsilon \sim \mathcal{N}(0, I)$, we can get the noisy sample as:

$$\hat{x}_t = \sqrt{\bar{\alpha}_t}x_t + \sqrt{1 - \bar{\alpha}_t}\epsilon \quad (8)$$

This process provides multi-scale noise perturbations for subsequent adversarial training, enhancing the robustness of the model.

Discriminator. DISCRIMINATOR D is encouraged to distinguish real and fake samples after SCHEDULER DIFFUSION, the DISCRIMINATOR loss is defined as:

$$\mathcal{L}_D = \frac{1}{2}(\text{BCE}(D(\hat{x}), 0) + \text{BCE}(D(x), 1)) \quad (9)$$

where $\text{BCE}(\cdot)$ is binary cross entropy.

Generator. GENERATOR G_θ is designed to learn complex correlations among spatiotemporal inputs, covariates, and salinity, enabling accurate imputation. After reversible normalization and positional encoding, the input \mathbf{X} is processed by a multi-level linear feature extractor (FE) and an attention module (Attn), yielding

$$\hat{s} = G_\theta \left(\text{Attn}(\text{FE}(\gamma \frac{\mathbf{X} - \mu}{\sqrt{\sigma^2 + \epsilon}} + \beta)) \right). \quad (10)$$

The GENERATOR's objective comprises two components: **Reconstruction loss**, which drives the generated salinity \hat{s}_i toward the true value s_i . **Feature-matching loss**, which encourages the DISCRIMINATOR's hidden activations for fake samples to align with those of real samples. Formally,

$$\mathcal{L}_G = \underbrace{\frac{1}{N} \sum_{i=1}^N (s_i - \hat{s}_i)^2}_{\text{MSE term}} + \underbrace{\frac{1}{M} \sum_{j=1}^M \|f_{\text{real},j} - f_{\text{fake},j}\|_1}_{\text{feature-matching term}}, \quad (11)$$

where f_{real} and f_{fake} denote the DISCRIMINATOR's feature vectors at a chosen hidden layer for real and generated samples, respectively.

Adversarial Objective. The overall training objective is formulated as a minimax game between the GENERATOR G and the DISCRIMINATOR D :

$$\min_G \max_D V(D, G), \quad (12)$$

where

$$V(D, G) = \underbrace{\mathbb{E}_{x \sim p_{\text{data}}} [\log D(x)]}_{\text{Encourage } D \text{ to correctly classify real samples}} + \underbrace{\mathbb{E}_{X \sim p_X, t} [\log(1 - D(q_t(G(X))))]}_{\text{Encourage } D \text{ to correctly identify generated samples}}. \quad (13)$$

4 Experiments

4.1 Datasets

We evaluate OASIS on two drifter datasets filtered to retain only coastal and nearshore data. Their key statistics are summarized in Table 1, with details as follows:

FP Observed is a real-world drifter dataset collected by the Harbor Branch Oceanographic Institute (HBOI) at Florida Atlantic University. Data were over six non-consecutive days using 2–3 drifters per day. Deployment and retrieval times varied across days, yielding a total of 109 trajectories. After preprocessing to remove anomalies, we retain three valid days (Dec 8, 2015; Dec 15, 2015; and Jun 16, 2016), resulting in 36 trajectories with 17,475 data points. For this study, we focus on Jun 16, 2016, which includes 4 trajectories with 11,426 salinity measurements near Fort Pierce Inlet, Florida, USA.

GoM Simulated is a synthetic drifter dataset generated by HBOI using a numerical ocean current model. The full dataset covers the Gulf of Mexico (Gulf of America) and adjacent waters, comprising 200 simulated drifter trajectories with 2,569 data points each, spanning from Oct 1, 2021, to Jan 16, 2022. To support our focus on salinity interpolation in sparsely sampled regions, we extract a subset near the Mississippi River delta, containing 69 trajectories and 52,253 time steps. This subset is divided into three monthly segments, **GoM-10** (Oct), **GoM-11** (Nov), and **GoM-12** (Dec).

4.2 Baselines

We compare OASIS with five representative baselines spanning statistical and deep learning methods to evaluate its performance: **Kriging** [8]: A classical geostatistical interpolation method that estimates unobserved values based on spatial autocorrelation. It is widely applied in environmental modeling.

Geographically Weighted Regression (GWR) [5]: A spatial regression model that fits local linear models at each location, capturing spatially varying relationships.

Multilayer Perceptron (MLP): A feedforward neural network that models nonlinear mappings from spatiotemporal features to salinity values.

Long Short-Term Memory (LSTM) [16]: A recurrent neural network designed to capture temporal dependencies, improving the model’s ability to reflect salinity dynamics over time.

Generative Adversarial Network (GAN) [12]: A generative model with a discriminator and generator trained adversarially. The generator learns to produce salinity fields conditioned on spatiotemporal inputs, capturing complex high-order patterns.

4.3 Evaluation Settings

Dataset. For each dataset, trajectories are randomly split into training (70%), validation (15%), and testing (15%) sets. To ensure consistent comparisons across all models, the random seed is fixed to 42, so that the same trajectories are used in each split.

Metrics. Model performance is evaluated using three regression metrics: Mean Absolute Error (MAE), $\frac{1}{N} \sum_{i=1}^N |y_i - \hat{y}_i|$; Root Mean Squared Error (RMSE), $\sqrt{\frac{1}{N} \sum_{i=1}^N (y_i - \hat{y}_i)^2}$; and Mean Absolute Percentage Error (MAPE), $\frac{100\%}{N} \sum_{i=1}^N \left| \frac{y_i - \hat{y}_i}{y_i} \right|$.

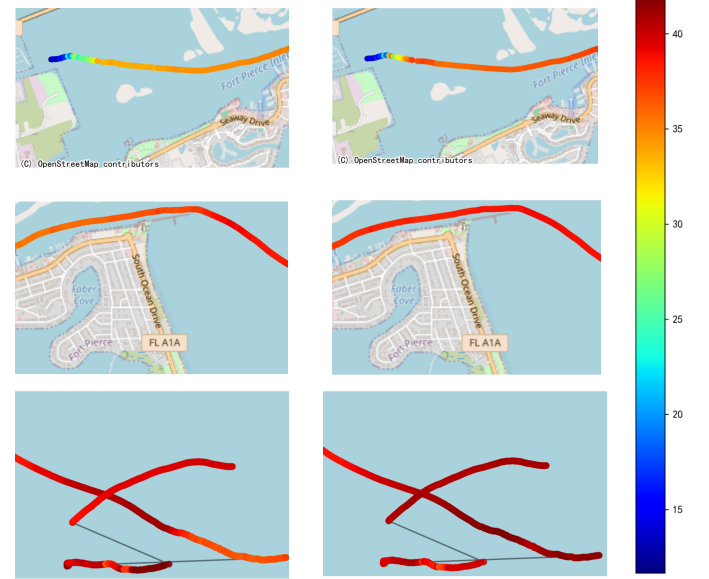


Figure 2: Comparison of sea surface salinity (psu) along drifter tracks in the FP Observed area. Left: True salinity measurements and Right: OASIS-imputed salinity fields.

4.4 Quantitative and Visual Results

Table 2 presents a comprehensive comparison of key performance metrics between OASIS and various baseline methods. OASIS consistently achieves superior performance, especially on the real-world FP Observed dataset. Compared to the best-performing baseline (MLP), OASIS reduces MAE by 3.8%, RMSE by 21.3%, and MAPE by 18.5%, highlighting its robustness and imputation accuracy.

Traditional methods such as Kriging exhibit the highest errors, highlighting their limitations in handling complex ocean dynamics. Although learning-based baselines exhibit improved performance, they still fall short in capturing intricate spatiotemporal dependencies, particularly under real-world data sparsity and noise. In some GoM datasets, MLP performs comparably well in MAPE, likely due to the smoother nature of synthetic trajectories, which can favor simpler architectures. However, these isolated gains do not generalize to real settings. In contrast, OASIS consistently delivers strong results across both real and synthetic datasets, demonstrating its ability to model intricate spatiotemporal structures.

Figure 2 visualizes salinity distributions in the FP Observed dataset, comparing (a) ground truth and (b) OASIS’s imputation.

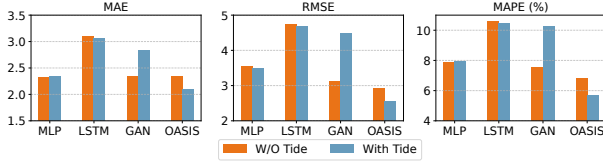
Table 1: Datasets characteristics

Datasets	# of trajectories	# of time steps	Datetime	Lon / Lat Range (°)	Salinity Range (psu)
FP Observed	4	11,426	16 Jun. 2016	[-80.32, -80.26] / [27.46, 27.47]	[06.82, 42.00]
GoM-10	53	21,847	Oct. 2021	[-91.63, -82.81] / [26.01, 30.34]	[30.12, 36.51]
GoM-11	41	9878	Nov. 2021	[-91.63, -82.65] / [26.01, 30.34]	[29.29, 36.13]
GoM-12	28	13,573	Dec. 2021	[-91.63, -82.65] / [26.01, 30.21]	[32.90, 36.30]

Table 2: The results in different study regions and times.

Model	FP Observed			GoM-10			GoM-11			GoM-12		
	MAE	RMSE	MAPE	MAE	RMSE	MAPE	MAE	RMSE	MAPE	MAE	RMSE	MAPE
Kriging	16.3373	20.8742	43.27%	0.8235	1.9499	2.50%	1.0416	1.7759	3.26%	1.5211	1.8672	2.50%
GWR	8.8916	19.1230	34.16%	2.2176	6.8032	6.90%	1.1731	2.9864	3.50%	0.8039	1.2283	2.30%
MLP	2.4257	3.7254	8.38%	0.3871	0.5031	1.15%	0.3525	0.5436	1.03%	0.3696	0.7539	1.07%
LSTM	3.0902	4.7452	10.57%	0.3980	0.5848	1.20%	0.3814	0.6539	1.13%	0.4679	0.8769	1.36%
GAN	2.8360	4.4835	10.26%	0.4977	0.5742	1.63%	0.8586	1.0717	2.49%	0.4707	0.7883	1.36%
OASIS (Ours)	2.3331	2.9338	6.83%	0.3288	0.4247	1.29%	0.3088	0.4084	1.21%	0.4761	0.6395	1.37%

Both plots share the same projection and color scale. The reconstructed field by OASIS accurately reflects the increasing salinity gradient from inlet (blue–green) to nearshore (orange–red), validating its ability to capture large-scale spatial patterns despite sparse sampling. Overall, the results confirm that OASIS is a robust, generalizable solution for nearshore salinity imputation.

**Figure 3: Performance comparison of different models on the FP Observed dataset with and without the tide feature.**

4.5 Covariate Analysis

To estimate salinity more accurately, certain physical covariates, such as velocity, sea surface temperature, wind speed, and density, can be leveraged via control equations [31]. However, these variables typically require in situ measurements and are thus impractical in many nearshore deployments. To address this limitation, we incorporate tidal height as a low-cost, easily accessible proxy, retrievable from NOAA databases or astronomical models without additional instrumentation. For each dataset, we locate the nearest NOAA Tides and Currents station and retrieve the corresponding tide information. Typically, 2–4 tide events are recorded per day. A sinusoidal function is fitted, either daily or monthly, based on these events, enabling continuous estimation of tide levels for each timestamp in the dataset. Figure 3 reports the imputation performance on the FP Observed dataset with and without the tide feature. We observe three main findings: **(1) Marginal gains for simple regressors.** Adding tide to MLP yields only minor RMSE reductions, with negligible MAE or MAPE improvement. Similar trends are seen for LSTM, indicating insufficient capacity to exploit the periodic tidal signal. **(2) Inconsistency in vanilla GAN.** Naïvely appending tide to the standard GAN degrades performance across all metrics.

This suggests that without an explicit mechanism to integrate the covariate, the added feature acts as noise, disrupting the adversarial learning dynamics. **(3) Effective integration in our Diffusion Adversarial Network variant.** By contrast, our framework leverages tide information through a dedicated conditioning module, yielding substantial improvements. These gains demonstrate that tide, as an easily observed proxy for unmeasured covariates, can be effectively exploited by models designed to capture its periodic structure.

In summary, while tide feature provide minimal benefit to generic models and may mislead unstructured GANs, our design successfully integrates this covariate, demonstrating both improved accuracy and robustness in salinity imputation.

Table 3: The result of ablation on FB Observed dataset. Norm, GDC, and SD are normalization, Global Dependency Capturing, and Scheduler Diffusion model, respectively.

Method	MAE	RMSE	MAPE
OASIS	2.3331	2.9338	6.83%
w/o Norm	2.4522	3.2500	7.15%
w/o GDC	2.7115	3.6371	8.88%
w/o SD	2.5280	3.4546	8.46%

4.6 Ablation Study

To quantify the contributions of each component in OASIS, we conduct an ablation study on the FB Observed dataset (Table 3). We remove normalization (Norm), the global dependency capturing module (GDC), and the scheduler diffusion model (SD) in turn, and report MAE, MSE, and MAPE. **(1) Without Norm.** Omitting the normalization step increases MAE from 2.3331 to 2.4522 (+5.1%), RMSE from 2.9338 to 3.2500 (+10.8%), and MAPE from 6.83% to 7.15%. This highlights the importance of feature scaling in stabilizing training and reducing bias. **(2) Without GDC.** Removing the global dependency capturing module leads to the largest performance degradation (MAE = 2.7115, +16.3%; RMSE = 3.6371, +24.0%; MAPE = 8.88%), demonstrating that modeling long-range spatial-temporal

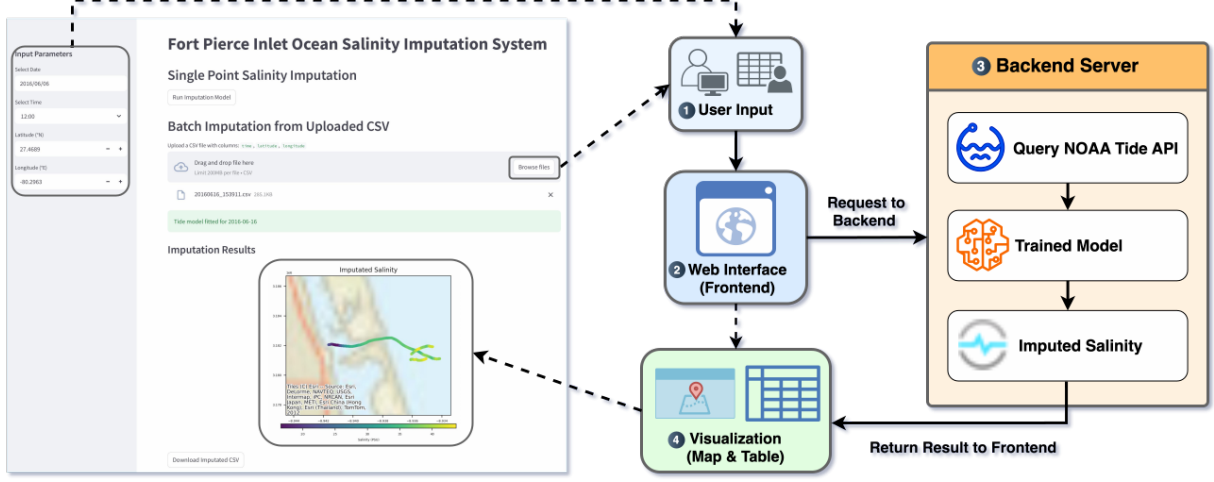


Figure 4: Overview of our OASIS: the web-based deployment interface (left) and the underlying system architecture (right).

correlations is critical for accurate salinity imputation. **(3) Without SD.** Excluding the scheduler diffusion component also worsens results (MAE = 2.5280, +8.4%; RMSE = 3.4546, +17.7%; MAPE = 8.46%), indicating that progressive refinement via diffusion scheduling effectively enhances the generator’s output quality.

These results confirm that each module—normalization, global dependency capturing, and scheduler diffusion contributes substantially to the overall performance of OASIS.

5 Application Deployment

To demonstrate the practical utility of OASIS, we developed a web-based deployment system for on-demand salinity imputation near Fort Pierce Inlet, as shown in Figure 4. The interface supports both single-point and batch imputation via interactive input of specific timestamps and coordinates or CSV upload.

The system is implemented with Streamlit (frontend) and PyTorch (backend). Upon receiving user input, the system queries the NOAA CO-OPS API to retrieve tide predictions for Fort Pierce Inlet (station ID: 8722212) on the specified date. A sinusoidal model is then fitted to the daily tide data and used to estimate the tide level at each queried timestamp.

The estimated tide levels, along with the spatiotemporal meta-data, are passed into the pre-trained model to generate imputed salinity values at each target location. The results are presented through a table and a geospatial visualization, where salinity levels are represented using a continuous color scale. The backend is modular and version-controlled. Updated models can be integrated into the deployment pipeline simply by replacing the serialized PyTorch model file (.pt) and its corresponding scaler (.pkl) without modifying the application logic. This enables continuous refinement of the imputation capability without disrupting the user experience.

The current deployment is lightweight and suitable for prototyping and small-scale use. To support broader accessibility and scalability, future versions will migrate to a more robust web architecture (e.g., React or Flask-React) with asynchronous interaction

capabilities. The system will also be deployed in cloud environments (e.g., AWS) using Docker to enable scalable, containerized services.

6 Conclusion

In this paper, we presented OASIS, a novel diffusion adversarial framework for sea salinity imputation that unifies reversible instance normalization, transformer-based global dependency modeling, and a scheduler-guided Adversarial Diffusion Network. By leveraging easily observed tidal height as an auxiliary covariate, OASIS is able to capture both large-scale gradients and fine-scale temporal fluctuations without requiring specialized instrumentation. Extensive quantitative experiments show consistent improvements over classical and neural baselines across benchmarks. Ablation studies confirm the essential roles of normalization, global dependency capturing, and the diffusion scheduler. Qualitative visualizations further illustrate OASIS’s ability to reconstruct smooth, continuous salinity fields and preserve localized extrema under severe data sparsity. To support real-world use, a lightweight web-based system is developed to enable real-time salinity imputation via interactive and batch inputs, with integrated NOAA tide access and future support for cloud scalability.

Acknowledgments and Disclosure of Funding

This research is supported by the U.S. National Science Foundation and Australia CSIRO joint project: NSF-CSIRO: Towards Interpretable and Responsible Graph Modeling for Dynamic Systems (IIS-2302786). This work has also been supported by the Australian Research Council (ARC) under grants FT210100097 and DP240101547.

GenAI Usage Disclosure

The authors confirm that all core research activities—including study design, data collection, analysis, and interpretation—were conducted without the use of generative artificial intelligence tools. Generative AI was employed only in a limited capacity during manuscript preparation: specifically for debugging minor coding errors,

and for grammar, spelling, and stylistic checks. No substantive content, scientific ideas, or interpretations were generated by AI, and all results, figures, and methodological descriptions reflect the authors' own work and expertise.

References

- [1] Laith Alzubaidi, Jinshuai Bai, Aiman Al-Sabaawi, Jose Santamaria, Ahmed Shihab Albahri, Bashar Sami Nayyef Al-Dabbagh, Mohammed A Fadhel, Mohamed Manoufali, Jinglan Zhang, Ali H Al-Timemy, et al. 2023. A survey on deep learning tools dealing with data scarcity: definitions, challenges, solutions, tips, and applications. *Journal of Big Data* 10, 1 (2023), 46.
- [2] Saqib Ejaz Awan, Mohammed Bennamoun, Ferdous Sohel, Frank Sanfilippo, and Girish Dwivedi. 2021. Imputation of missing data with class imbalance using conditional generative adversarial networks. *Neurocomputing* 453 (2021), 164–171.
- [3] Lorenzo Beretta and Alessandro Santaniello. 2016. Nearest neighbor imputation algorithms: a critical evaluation. *BMC medical informatics and decision making* 16 (2016), 197–208.
- [4] NA Bray. 1988. Water mass formation in the Gulf of California. *Journal of Geophysical Research: Oceans* 93, C8 (1988), 9223–9240.
- [5] Chris Brunson, A Stewart Fotheringham, and Martin E Charlton. 1996. Geographically weighted regression: a method for exploring spatial nonstationarity. *Geographical analysis* 28, 4 (1996), 281–298.
- [6] Luca R Centurioni, Verena Hormann, Yi Chao, Gilles Reverdin, Jordi Font, and Dong-Kyu Lee. 2015. Sea surface salinity observations with Lagrangian drifters in the tropical North Atlantic during SPURS: Circulation, fluxes, and comparisons with remotely sensed salinity from Aquarius. *Oceanography* 28, 1 (2015), 96–105.
- [7] Astha Chawla, Prakhar Agrawal, Bijaya Ketan Panigrahi, and Kolin Paul. 2023. Deep-learning-based data-manipulation attack resilient supervisory backup protection of transmission lines. *Neural Computing and Applications* 35, 7 (2023), 4835–4854.
- [8] Kai Chen, Minjie Ni, Minggang Cai, Jun Wang, Dongren Huang, Huorong Chen, Xiao Wang, and Mengyang Liu. 2016. Optimization of a coastal environmental monitoring network based on the Kriging method: A case study of Quanzhou Bay, China. *BioMed research international* 2016, 1 (2016), 7137310.
- [9] Eugenio Cutolo, Ananda Pascual, Simon Ruiz, Nikolaos D Zarokanellos, and Roman Fablet. 2024. CLOINet: ocean state reconstructions through remote-sensing, in-situ sparse observations and deep learning. *Frontiers in Marine Science* 11 (2024), 1151868.
- [10] Grace Deng, Cuize Han, and David S Matteson. 2022. Extended missing data imputation via GANs for ranking applications. *Data Mining and Knowledge Discovery* 36, 4 (2022), 1498–1520.
- [11] Weiwei Fu, Jun She, and Shiyu Zhuang. 2011. Application of an Ensemble Optimal Interpolation in a North/Baltic Sea model: Assimilating temperature and salinity profiles. *Ocean Modelling* 40, 3-4 (2011), 227–245.
- [12] Ian J Goodfellow, Jean Pouget-Abadie, Mehdi Mirza, Bing Xu, David Warde-Farley, Sherjil Ozair, Aaron Courville, and Yoshua Bengio. 2014. Generative adversarial nets. *Advances in neural information processing systems* 27 (2014).
- [13] Nicolas Guillou, Georges Chapalain, and Sébastien Petton. 2023. Predicting sea surface salinity in a tidal estuary with machine learning. *Oceanologia* 65, 2 (2023), 318–332.
- [14] Shengnan Guo, Tonglong Wei, Yiheng Huang, Miaomiao Zhao, Ran Chen, Yan Lin, Youfang Lin, and Huaiyu Wan. 2024. An Experimental Evaluation of Imputation Models for Spatial-Temporal Traffic Data. arXiv:2412.04733 [cs.LG] <https://arxiv.org/abs/2412.04733>
- [15] Michael Hahn. 2020. Theoretical limitations of self-attention in neural sequence models. *Transactions of the Association for Computational Linguistics* 8 (2020), 156–171.
- [16] Sepp Hochreiter and Jürgen Schmidhuber. 1997. Long short-term memory. *Neural computation* 9, 8 (1997), 1735–1780.
- [17] Verena Hormann, Luca R Centurioni, and Gilles Reverdin. 2015. Evaluation of drifter salinities in the subtropical North Atlantic. *Journal of Atmospheric and Oceanic Technology* 32, 1 (2015), 185–192.
- [18] Uiwon Hwang, Dahuin Jung, and Sungroh Yoon. 2019. Hexagon: Generative adversarial nets for real world classification. In *International conference on machine learning*. PMLR, 2921–2930.
- [19] Xiaoyan Jia, Qiyang Ji, Lei Han, Yu Liu, Guoqing Han, and Xiayan Lin. 2022. Prediction of sea surface temperature in the East China Sea based on LSTM neural network. *Remote Sensing* 14, 14 (2022), 3300.
- [20] Nan Jiang, Yanan Li, Hua Zuo, Hui Zheng, and Qinghe Zheng. 2020. BiLSTM-A: A missing value imputation method for PM2.5 prediction. In *2020 2nd International Conference on Applied Machine Learning (ICAML)*. IEEE, 23–28.
- [21] Bora Jin, Amy H Herring, and David Dunson. 2024. Spatial predictions on physically constrained domains: applications to Arctic sea salinity data. *The Annals of Applied Statistics* 18, 2 (2024), 1596–1617.
- [22] Ming Jin, Guangsi Shi, Yuan-Fang Li, Qingsong Wen, Bo Xiong, Tian Zhou, and Shirui Pan. 2023. How expressive are spectral-temporal graph neural networks for time series forecasting? *arXiv preprint arXiv:2305.06587* (2023).
- [23] Taesung Kim, Jinhee Kim, Yunwon Tae, Cheonbok Park, Jang-Ho Choi, and Jaegul Choo. 2022. Reversible Instance Normalization for Accurate Time-Series Forecasting against Distribution Shift. In *International Conference on Learning Representations*. <https://openreview.net/forum?id=cGDakQo1C0p>
- [24] Yeo-Jin Kim and Min Chi. 2018. Temporal Belief Memory: Imputing Missing Data during RNN Training.. In *In Proceedings of the 27th International Joint Conference on Artificial Intelligence (IJCAI-2018)*.
- [25] Young Jun Kim, Daehyeon Han, Eunna Jang, Jungho Im, and Taejun Sung. 2023. Remote sensing of sea surface salinity: challenges and research directions. *GI-Science & Remote Sensing* 60, 1 (2023), 2166377.
- [26] Tuyen Pham Le, Cheolkyun Rho, Yelin Min, Sungreong Lee, and Daewoo Choi. 2021. A2GAN: A deep reinforcement-based learning algorithm for risk-aware in finance. *IEEE Access* 9 (2021), 137165–137175.
- [27] Jiyue Li, Senzhang Wang, Jiaqiang Zhang, Hao Miao, Junbo Zhang, and Philip S Yu. 2022. Fine-grained urban flow inference with incomplete data. *IEEE Transactions on Knowledge and Data Engineering* 35, 6 (2022), 5851–5864.
- [28] Xiao Li, Huan Li, Harry Kai-Ho Chan, Hua Lu, and Christian S Jensen. 2023. Data imputation for sparse radio maps in indoor positioning. In *2023 IEEE 39th International Conference on Data Engineering (ICDE)*. IEEE, 2235–2248.
- [29] Meiling Liu, Xiangnan Liu, Jiale Jiang, and Xiaopeng Xia. 2013. Artificial neural network and random forest approaches for modeling of sea surface salinity. *International Journal of Remote Sensing Applications* 3, 4 (2013), 229–235.
- [30] Yixin Liu, Thalaiyasingam Ajanthan, Hisham Husain, and Vu Nguyen. 2024. Self-supervision improves diffusion models for tabular data imputation. In *Proceedings of the 33rd ACM International Conference on Information and Knowledge Management*. 1513–1522.
- [31] Trevor J McDougall, Paul M Barker, Ryan M Holmes, Rich Pawlowicz, Stephen M Griffies, and Paul J Durack. 2021. The interpretation of temperature and salinity variables in numerical ocean model output and the calculation of heat fluxes and heat content. *Geoscientific Model Development* 14, 10 (2021), 6445–6466.
- [32] Oleg Melnichenko, Peter Hacker, Nikolai Maximenko, Gary Lagerloef, and James Potemra. 2014. Spatial optimal interpolation of Aquarius sea surface salinity: Algorithms and implementation in the North Atlantic. *Journal of Atmospheric and Oceanic Technology* 31, 7 (2014), 1583–1600.
- [33] Oleg Melnichenko, Peter Hacker, Nikolai Maximenko, Gary Lagerloef, and James Potemra. 2016. Optimum interpolation analysis of a quarius sea surface salinity. *Journal of Geophysical Research: Oceans* 121, 1 (2016), 602–616.
- [34] Till Rötting, Stacey M Trevathan-Tackett, Christian R Voolstra, Cliff Ross, Samuel Chaffron, Paul J Durack, Laura M Warmuth, and Michael Sweet. 2023. Human-induced salinity changes impact marine organisms and ecosystems. *Global change biology* 29, 17 (2023), 4731–4749.
- [35] Matthew W Schmidt, Howard J Spero, and David W Lea. 2004. Links between salinity variation in the Caribbean and North Atlantic thermohaline circulation. *Nature* 428, 6979 (2004), 160–163.
- [36] Xu Shen, Yixin Liu, Yiwei Dai, Yili Wang, Rui Miao, Yue Tan, Shirui Pan, and Xin Wang. 2025. Understanding the Information Propagation Effects of Communication Topologies in LLM-based Multi-Agent Systems. *arXiv preprint arXiv:2505.23352* (2025).
- [37] Katie Smyth and Mike Elliott. 2016. Effects of changing salinity on the ecology of the marine environment. *Stressors in the marine environment: physiological and ecological responses; societal implications* (2016), 161–174.
- [38] Tao Song, Ziheng Wang, Pengfei Xie, Nisheng Han, Jingyu Jiang, and Danya Xu. 2020. A novel dual path gated recurrent unit model for sea surface salinity prediction. *Journal of Atmospheric and Oceanic Technology* 37, 2 (2020), 317–325.
- [39] Lizhuang Tan, Wei Su, Wei Zhang, Huiling Shi, Jingying Miao, and Pilar Manzanares-Lopez. 2021. A packet loss monitoring system for in-band network telemetry: detection, localization, diagnosis and recovery. *IEEE Transactions on Network and Service Management* 18, 4 (2021), 4151–4168.
- [40] Olga Troyanskaya, Michael Cantor, Gavin Sherlock, Pat Brown, Trevor Hastie, Robert Tibshirani, David Botstein, and Russ B Altman. 2001. Missing value estimation methods for DNA microarrays. *Bioinformatics* 17, 6 (2001), 520–525.
- [41] George Veronis. 1972. On properties of seawater defined by temperature, salinity, and pressure. (1972).
- [42] Elena Voita, David Talbot, Fedor Moiseev, Rico Sennrich, and Ivan Titov. 2019. Analyzing multi-head self-attention: Specialized heads do the heavy lifting, the rest can be pruned. *arXiv preprint arXiv:1905.09418* (2019).
- [43] Yufeng Wang, Dan Li, Xiang Li, and Min Yang. 2021. PC-GAIN: Pseudo-label conditional generative adversarial imputation networks for incomplete data. *Neural Networks* 141 (2021), 395–403.
- [44] FA Whitney, WR Crawford, and PJ Harrison. 2005. Physical processes that enhance nutrient transport and primary productivity in the coastal and open ocean of the subarctic NE Pacific. *Deep Sea Research Part II: Topical Studies in Oceanography* 52, 5-6 (2005), 681–706.
- [45] Jinsung Yoon, William R Zame, and Mihaela Van Der Schaar. 2018. Deep sensing: Active sensing using multi-directional recurrent neural networks. In *International*

- Conference on Learning Representations*.
- [46] Seongwook Yoon and Sanghoon Sull. 2020. GAMIN: Generative adversarial multiple imputation network for highly missing data. In *Proceedings of the IEEE/CVF conference on computer vision and pattern recognition*. 8456–8464.
 - [47] Lisan Yu. 2011. A global relationship between the ocean water cycle and near-surface salinity. *Journal of Geophysical Research: Oceans* 116, C10 (2011).
 - [48] Xinlu Zhang, Shiyang Li, Zhiyu Chen, Xifeng Yan, and Linda Ruth Petzold. 2023. Improving medical predictions by irregular multimodal electronic health records modeling. In *International Conference on Machine Learning*. PMLR, 41300–41313.
 - [49] He Zhao, Ke Sun, Amir Dezfouli, and Edwin V Bonilla. 2023. Transformed distribution matching for missing value imputation. In *International Conference on Machine Learning*. PMLR, 42159–42186.
 - [50] Xin Zheng, Wei Huang, Chuan Zhou, Ming Li, and Shirui Pan. 2025. Test-Time Graph Neural Dataset Search With Generative Projection. In *Forty-second International Conference on Machine Learning*.
 - [51] Xin Zheng, Dongjin Song, Qingsong Wen, Bo Du, and Shirui Pan. 2024. Online GNN Evaluation Under Test-time Graph Distribution Shifts. In *The Twelfth International Conference on Learning Representations*.
 - [52] Xin Zheng, Miao Zhang, Chunyang Chen, Soheila Molaei, Chuan Zhou, and Shirui Pan. 2024. GnnEvaluator: Evaluating gnn performance on unseen graphs without labels. *Advances in Neural Information Processing Systems* 36 (2024).
 - [53] Xin Zheng, Miao Zhang, Chunyang Chen, Quoc Viet Hung Nguyen, Xingquan Zhu, and Shirui Pan. 2024. Structure-free graph condensation: From large-scale graphs to condensed graph-free data. *Advances in Neural Information Processing Systems* 36 (2024).
 - [54] Xu Zhou, Xiaofeng Liu, Gongjin Lan, and Jian Wu. 2021. Federated conditional generative adversarial nets imputation method for air quality missing data. *Knowledge-Based Systems* 228 (2021), 107261.